Mn and Fe *K*-edge XAS Spectra of Manganese and Iron Nitrido Compounds

Rainer Niewa,*[a] Zhiwei Hu,[b] and Rüdiger Kniep[a]

Keywords: X-ray absorption spectroscopy / Nitrides / Iron / Manganese

We performed a Mn *K*-edge XAFS study of a number of highly moisture-sensitive nitridomanganates with manganese in different oxidation states and in various surroundings: $Li_2[(Li_{1-x}Mn^{I}_{x})N]$ [$x = 0.75(1)$], $Li_{24}[Mn^{III}N_3]_3N_2$, and $Li_7[Mn^{V}N_4]$. For reference purposes Mn, MnO and θ-Mn_6N_{5+x} [$x = 0.26(1)$] were measured. The energy positions of the pre-edge maxima are almost independent of the electronic state of Mn, while the intensity is sensitive to the geometric arrangement of the coordination of Mn. The main-edge is sensitive to the oxidation state – a clear shift to higher energies with increasing oxidation state can be seen. This shift is smaller than the shift observed for the corresponding oxides, due to the lower electronegativity of nitrogen compared to oxygen, and corresponds to a higher covalency of the Mn–N bond. Similar results can be taken from the Fe *K*-edges of $Li_2[(Li_{1-x}Fe^{I}_{x})N]$ with $x = 0.20(1)$ and $Li_3[Fe^{III}N_2]$ in comparison to metallic Fe, $Fe^{II}SO_4{\cdot}7H_2O$ and α-$Fe^{III}_2O_3$. The results are consistent with the presence of an unusual oxidation state (+1) for the transition metals in the phases of the general composition $Li_2[(Li_{1-x}M_x)N]$.

Introduction

XAS spectroscopy at the thresholds is an element-specific tool that can provide valuable information on the oxidation state and the electronic configuration of most atomic components of both crystalline and amorphous materials. The shape and energy position of the absorption spectrum in its near-edge region is closely related to the electronic structure, and is partly also influenced by the magnetic state, the local symmetry, and the coordination environment of the nuclei, while the oscillation observed in the high energy region of the spectrum is associated with the arrangement of the atoms, i.e. the local surrounding.

A wide range of oxidation states is known for Mn: in inorganic oxide compounds manganese covers the whole range of oxidation states from +2 to +7, and in carbonyl complexes the oxidation states −1, 0 and +1 are also known. In nitride chemistry, the highest reported oxidation state for manganese is +5, while the lower oxidation states are predominately stabilized (as generally in 3d nitridometalates):[1] oxidation states below +2 are frequently observed. The oxidation state +5 is known only for $Li_7[MnN_4]$,[2] with a high ratio of electropositive elements to manganese, while in binary manganese nitrides even +3 has not been reached so far. MnN reported in the literature always exhibits a nitrogen deficiency and belongs to the θ-Mn_6N_{5+x} phase region.[3] The situation is similar for lithium nitridoferrates: $Li_3[FeN_2]$ contains iron in its highest oxidation state (+3) observed so far in nitride chemistry.[4] $Li_4[Fe^{II}N_2]$[5] and $Li_2[(Li_{1-x}Fe^{I}_{x})N]$[6,7] are formed as decomposition phases from $Li_3[Fe^{III}N_2]$ at elevated temperatures.

In XAS at the transition metal *K*-edge an M 1s core-electron is excited to the 4p orbitals (dipole allowed), at higher energy the M 1s core-electron is excited to the continuum. In general, XAS spectra of the first-row transition metals have a weak pre-edge structure about 10 eV below the absorption edge, a feature that was assigned as originating from a 1s→3d transition.[8−10] For compounds with the transition metal in a centrosymmetric environment, a 1s→3d transition is electric dipole-forbidden by parity considerations. (The fact, that dipole selection rules hold only in systems with an inversion center is known in spectroscopy as Laporte's rule[11]). However, a weak pre-edge feature is still observed experimentally. In the case of non-centrosymmetric local surroundings M-4p-wavefunctions can mix into the 3d orbitals which provides some electric dipole-allowed 1s→4p character to the transition. All this may lead to a significant pre-edge feature that is more intense for local symmetries lacking an inversion center. In particular, the features in the region of the 1s→3d transition have been shown to be sensitive to the oxidation state and coordination geometry of a 3d transition metal.[10]

X-ray absorption probes the unoccupied part of the electronic structure of the system. Thus, for all discussions it should be mentioned that information on the ground state is concluded from excited states with an M 1s hole, a conclusion which might not be uncritical. This situation is

---

[a] Max-Planck-Institut für Chemische Physik fester Stoffe,
Nöthnitzer Str. 40, 01187 Dresden, Germany
Fax: (internat.) +49-(0)351/4646-3002
E-mail: niewa@cpfs.mpg.de
[b] II. Physikalisches Institut der Universität zu Köln,
Zülpicher Str. 77, 50937 Köln, Germany

moderated for metallic compounds, since, as a general rule, the core holes in metals are better screened than in insulators, therefore many-body effects involving both the core hole and the excited electron are less important for metals.[8] We chose to measure *K*-edge spectra, because: i) the relevant energies make it possible to work in transmission mode, hence to use fully encapsulated samples (necessary for the strongly sensitive compounds), and ii) the valence state can be taken directly from the energy shift of the main absorption edge, while in $L_{2,3}$ XAS spectra the edge of oxidized 3d metals can lie at higher or lower energies than those of the corresponding metallic elements. The latter fact is due to strong multiplet interactions in the final state effects.[12,13]

Results and Discussion

The striking features of the presented data are the pre-edge peaks visible for all investigated nitrides, although their shape and their intensity are significantly different. As can be seen from Figure 1, for the manganese compounds the most pronounced and best separated pre-edge features are visible for $Li_7[Mn^{V}N_4]$ and $Li_{24}[Mn^{III}N_3]_3N_2$ around 6539 eV. This pre-edge peak was assigned to a 1s→3d transition.[8−10] In the spectra of the other nitrides the pre-edge is observed only as a shoulder of the main absorption edge, which itself reflects a 1s→4p transition. The positions of the pre-edge feature exhibit only a slight change in energy in the presented data. Therefore, the pre-edge peak becomes more visible when the main absorption edge shifts to higher energies. It was observed earlier that the pre-edge peaks are shifted to higher energy with increasing oxidation state for chromium oxides.[14,15] Such a shift can only be confirmed for the well-separated strong pre-edge signals in the spectra of $Li_7[Mn^{V}N_4]$ and $Li_{24}[Mn^{III}N_3]_3N_2$, indicating the difference in oxidation state (about 1 eV). The intensity of the pre-edge peak can be related directly to the local symmetry of the manganese coordination in the different nitrido compounds: $Li_7[Mn^{V}N_4]$: tetrahedral, lacking centrosymmetry,[2] $Li_{24}[Mn^{III}N_3]_3N_2$: trigonal, slightly non-planar, lacking centrosymmetry,[2] $Li_2[(Li_{1-x}Mn^{I}_{x})N]$: linear by N, and thus centrosymmetric, but with Li-Mn disorder in the basal plane perpendicular to the Mn−N bond (second coordination sphere assembled from six Li or Mn) breaking the symmetry,[2] θ-Mn_6N_{5+x}: octahedral, centrosymmetric, but with some degree of N-vacancies breaking the local symmetry.[3]

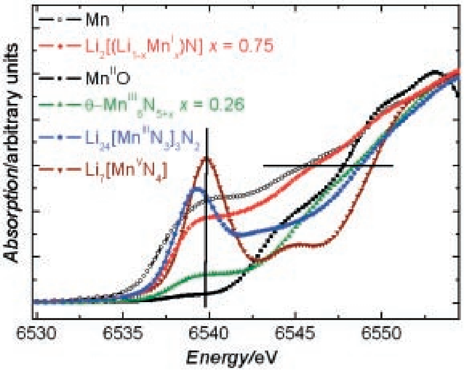

Figure 1. Near-edge XAS spectra of Mn, $Li_2[(Li_{1-x}Mn^{I}_{x})N]$ (x = 0.75), $Mn^{II}O$, θ-Mn_6N_{5+x} (x = 0.26), $Li_{24}[Mn^{III}N_3]_3N_2$ and $Li_7[Mn^{V}N_4]$; the strong pre-edge peak for the compounds lacking local centrosymmetry at the Mn-center and the shift of the main absorption edge to higher energies with increasing oxidation state are clearly visible

Unfortunately, the inflection point of the main absorption edge in many spectra is overlapped by the pre-edge feature. However, the general trend of the increasing absorption edge levels at about 0.6 of the full edge jump from elemental Mn and the Mn^{I}-phase $Li_2[(Li_{1-x}Mn^{I}_{x})N]$ to $Mn^{II}O$ is still visible (Figure 1). The inflection point of θ-Mn_6N_{5+x} (x = 0.26) lies slightly lower than that of $Li_{24}[Mn^{III}N_3]_3N_2$, indicating the lower oxidation state of Mn in the binary nitride due to the nitrogen deficiency in the crystal structure compared to the ideal composition for a manganese(III) nitride. The edge of $Li_7[Mn^{V}N_4]$ lies at the highest energy, as was to be expected. The absorption edge of $Mn^{II}O$ is much closer to that of the manganese(III) nitrido compounds than to that of the nitridomanganate(I). This is easily understood from the lower electronegativity of the nitrogen ligands compared to oxygen. As observed earlier, the absorption edge is shifted to higher energies with increasing electronegativity of the ligands.[16]

Larger degrees of vacancies and, thus, increased oxidation states of the transition metals in the sense of $Li_{2-y}[(Li_{1-x}M_x)N]$, have been discussed for the analogues substitution series of M = Cu, Ni and Co.[17−19] The small shift of the absorption edge of the manganese(I) compound compared to the manganese foil proves that the oxidation state of manganese in $Li_2[(Li_{1-x}Mn_x)N]$ is close to +1, indicating that the vacancy concentration in this phase (y in $Li_{2-y}[(Li_{1-x}Mn_x)N]$) is small. This is in agreement with our single crystal and magnetic susceptibility investigations.[2] Similar results were also obtained for the M = Cu, Ni, Co substitution phases from XAS spectroscopy, indicating oxidation states close to +1.[20]

The main absorption edge is determined by the threshold of the electron dipole transition from the manganese 1s orbital to the continuum of p-like states above the Fermi energy. The shift of the edge position is correlated with the length of the Mn−N bonds: the shorter it is, the larger the overlap between the electron wavefunctions originating from Mn and N. This results in an increase of the energy of the outer states relative to the energy of the core levels, and thus in a higher-energy shift of the absorption edge. Higher oxidation states generally lead to shorter bond lengths considering the same coordination geometry, thus adding to the effect of the positive edge shift. In our study lower coordination numbers (*CN*) in phases with lower oxidation states of M partly counteract these effects: $\bar{d}$(Mn−N): $Li_2[(Li_{1-x}Mn_x)N]$ [x = 0.75(1)] with *CN*(Mn) = 2: 191 pm;[2] $Li_{24}[MnN_3]_3N_2$ with *CN*(Mn) = 3: 178 pm;[2] $Li_7[MnN_4]$ with *CN*(Mn) = 4: 182 pm;[2] θ-Mn_6N_{5+x} (x = 0.26) with *CN*(Mn) = 5,6: 218 pm[3]. The effect of Li−Mn−disorder, i.e. the size of the substitution parameter

x, on the average bond length $\bar{d}$(Li,Mn−N) in $Li_2[(Li_{1-x}Mn_x)N]$ is negligible.[21]

Figure 2 plots the Fe K-edges of $Li_3[Fe^{III}N_2]$ and $Li_2[(Li_{1-x}Fe^{I}_x)N]$ [$x = 0.20(1)$] together with reference compounds and the element. As discussed for the manganese compounds, good separation of the pre-edge feature is only reached for $Li_3[Fe^{III}N_2]$ with Fe in tetrahedral (non-centrosymmetric) coordination. The main absorption edge taken at 0.6 of the total edge jump shifts only slightly from metallic Fe to $Li_2[(Li_{1-x}Fe^{I}_x)N]$ [$x = 0.20(1)$] indicating the oxidation state of iron in the latter phase is close to unity. The absorption edges of $Fe^{II}SO_4{\cdot}7H_2O$ and $Li_3[Fe^{III}N_2]$ nearly coincide for the same reason of electronegativity difference of nitrogen and oxygen as discussed above, while the Fe K-edge of α-$Fe^{III}_2O_3$ is clearly shifted to higher energies.

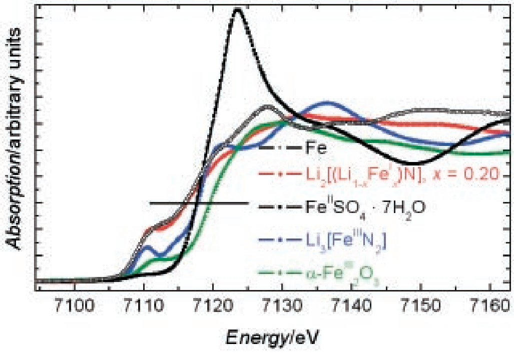

Figure 2. Near-edge XAS spectra of Fe, $Li_2[(Li_{1-x}Fe^{I}_x)N]$ ($x = 0.20$), $Fe^{II}SO_4{\cdot}7H_2O$, $Li_3[Fe^{III}N_2]$, and α-$Fe^{III}_2O_3$; the shift of the main absorption edge to higher energies with increasing oxidation state is clearly visible

Experimental Section

Samples of the compounds under investigation were prepared and characterized as described previously.[2,3,7,22] For the XAS measurements the air-sensitive compounds $Li_7[Mn^{V}N_4]$, $Li_{24}[Mn^{III}N_3]_3N_2$, $Li_2[(Li_{1-x}Mn^{I}_x)N]$ [$x = 0.75(1)$], $Li_3[Fe^{III}N_2]$ and $Li_2[(Li_{1-x}Fe^{I}_x)N]$ [$x = 0.20(1)$] were handled in an Ar-filled glove box with $p(O_2, H_2O) < 1$ ppm. All powder samples were mixed with three times their volume of dry B_4C to produce homogenous absorbers. The air-sensitive samples were loaded in steel capsules equipped with Be windows (0.5 mm). Due to the extreme moisture sensitivity of these samples and the necessary way of handling, thickness effects in the resulting XAS spectra are basically inevitable.[23,24] Non-sensitive samples (MnO, θ-Mn_6N_{5+x}, α-Fe_2O_3) were prepared on mylar films. $Fe^{II}SO_4{\cdot}7H_2O$ was also loaded into a steel capsule to prevent dehydration in vacuo.

The M K-edge measurements were performed in transmission geometry at the E4 bending magnet beamline located at the DORISIII storage ring in the HASYLAB laboratory (Hamburg, Germany). The X-ray beam outgoing from the bending magnet and formed with the toroidal and plane golden mirrors was monochromatized using a double crystal monochromator, equipped with a Si(111) crystal. This resulted in an experimental resolution of about 1.5 eV (FWHM) at the studied thresholds. For detectors ionization chambers were used. The absorption spectra were measured simultaneously with the spectrum of metallic manganese or iron foil, respectively, serving as references for energy calibration. Typical scan times were 30 min with smaller step size and longer measurement times in the range of the main-edge.

Acknowledgments

We wish to thank Dr. K. Klementiev for his support at the E4 beamline.

---

[1] R. Niewa, *Z. Kristallogr.* **2002**, *217*, 8−23.
[2] R. Niewa, F. R. Wagner, W. Schnelle, O. Hochrein, R. Kniep, *Inorg. Chem.* **2001**, *40*, 5215−5222.
[3] A. Leineweber, R. Niewa, H. Jacobs, W. Kockelmann, *J. Mater. Chem.* **2000**, *10*, 2827−2834.
[4] A. Gudat, R. Kniep, A. Rabenau, W. Bronger, U. Ruschewitz, *J. Less-Common Met.* **1990**, *161*, 31−36.
[5] A. Gudat, R. Kniep, A. Rabenau, *Angew. Chem.* **1991**, *103*, 217−218; *Angew. Chem. Int. Ed. Engl.* **1991**, *30*, 199−200.
[6] J. Klatyk, R. Kniep, *Z. Kristallogr. NCS* **1999**, *214*, 447−448.
[7] J. Klatyk, W. Schnelle, F. R. Wagner, R. Niewa, P. Nowak, R. Kniep, M. Waldeck, V. Ksenofontov, P. Gütlich, *Phys. Rev. Lett.* **2002**, *88*, 207202−1-4.
[8] L. A. Grunes, *Phys. Rev. B* **1983**, *27*, 2111−2131.
[9] F. M. F. de Groot, *J. Electron. Spectrosc. Relat. Phenom.* **1994**, *67*, 529−622.
[10] R. G. Shulman, Y. Yafet, P. Eisenberger, W. E. Blumberg, *Prog. Natl. Acad. Sci. USA* **1976**, *73*, 1384−1388.
[11] See, for example, P. J. Durrant, B. Durrant, *Introduction to Advanced Inorganic Chemistry*, 2nd ed., Longman Group, London, **1970**, p. 976.
[12] R. D. Leapman, L. A. Grunes, *Phys. Rev. Lett.* **1980**, *45*, 397−401.
[13] R. D. Leapman, L. A. Grunes, P. L. Fejes, *Phys. Rev. B* **1982**, *26*, 614−635.
[14] A. Pantelouris, G. Küper, J. Hourmes, C. Feldmann, M. Jansen, *J. Am. Chem. Soc.* **1995**, *117*, 11749−11753.
[15] Z. Hu, G. Kaindl, A. Hayer, D. Reinen, *Z. Anorg. Allg. Chem.* **2001**, *627*, 2647−2653.
[16] Z. Hu, G. Kaindl, G. Meyer, *J. Alloys Comp.* **1997**, *246*, 186−192.
[17] A. G. Gordon, D. H. Gregory, A. J. Blake, D. P. Weston, M. O. Jones, *Int. J. Inorg. Mater.* **2001**, *3*, 973−981.
[18] D. H. Gregory, P. M. O'Meara, A. G. Gordon, D. J. Siddons, A. J. Blake, M. G. Barker, T. A. Hamor, P. P. Edwards, *J. Alloys Comp.* **2001**, *317*, 237−244.
[19] M. T. Weller, S. E. Dann, P. F. Henry, D. B. Currie, *J. Mater. Chem.* **1999**, *9*, 283−287.
[20] R. Niewa, Z.-L. Huang, W. Schnelle, Z. Hu, R. Kniep, Z. Anorg. Allg. Chem. in press.
[21] J. Klatyk, R. Niewa, R. Kniep, *Z. Naturforsch., Teil B* **2000**, *55*, 988−991.
[22] F. Tessier, M. R. Rannade, A. Navrotsky, R. Niewa, F. J. DiSalvo, A. Leineweber, H. Jacobs, *Z. Anorg. Allg. Chem.* **2001**, *627*, 194−200.
[23] D. M. Pease, *Appl. Spectrosc.* **1976**, *30*, 405−410.
[24] F. Szmulowicz, D. M. Pease, *Phys. Rev. B* **1978**, *17*, 3341−3355.

Received January 9, 2003
[I03011]